available at www.sciencedirect.com

ScienceDirect

www.elsevier.com/locate/brainres

BRAIN RESEARCH

Research Report

Spinogenesis and pruning in the primary auditory cortex of the macaque monkey (*Macaca fascicularis*): An intracellular injection study of layer III pyramidal cells

Guy N. Elston[a,*], *Tsuguhisa Okamoto*[b], *Tomofumi Oga*[b], *Dimity Dornan*[c,d], *Ichiro Fujita*[b]

[a]*Centre for Cognitive Neuroscience, 60 Duke Rd, Doonan, Sunshine Coast, Queensland, 4562, Australia*
[b]*Graduate School of Frontier Biosciences, Osaka University, Machikaneyama 1-3, Toyonaka, Osaka 560-8531, Japan*
[c]*I HEAR Innovation Research Centre, Brisbane, Queensland, Australia*
[d]*Hear and Say Centre, Brisbane, Queensland, Australia*

ARTICLE INFO

Article history:
Accepted 18 December 2009
Available online 4 January 2010

Keywords:
Plasticity
Hebb
Dendrite
Spine
Maturation
Development

ABSTRACT

Recently we demonstrated that neocortical pyramidal cells in visual, visual association and prefrontal cortex of the macaque monkey are characterised by different growth, branching, spinogenesis and pruning during development. Some neurons, such as those in the primary visual area, prune more spines than they grow following sensory onset, while others such as those in area TE grow more than they prune. To what extent these different neuronal growth profiles may vary among cortical areas remains to be determined. To better comprehend the nature and extent of these regional differences in pyramidal cell growth profiles we expanded the bases for comparison by studying neurons in the primary auditory cortex (A1). We found that pyramidal cells in A1 continue to grow their basal dendritic trees beyond the peak period of spinogenesis ($3^1/_2$ months) up until at least 7 months of age. Likewise, the most prolific branching patterns were observed in the dendritic trees of pyramidal cells at 7 months of age. These data reveal that the basal dendritic trees of cells in A1 continue to grow for a much longer period, and attain almost double the number of spines, as compared with those in V1. Such differences in the growth profiles of neocortical pyramidal cells among cortical areas may influence therapeutic outcomes when applying new technologies such as neurotrophic delivery devices or stem cell therapy.

1. Introduction

The basal dendritic trees of pyramidal cells, which comprise more than 70% of all cortical neurons (DeFelipe and Fariñas, 1992), grow in size, extend and retract branches, and grow and prune spines at different rates among cortical areas in the macaque monkey. For example, the dendritic trees of pyramidal cells in the primary visual area (V1) are at their biggest at birth, and then decrease in size by 40% during the first $3^1/_2$ months of postnatal development (Elston et al., 2009a). Pyramidal cells in inferotemporal association cortex continue to grow from birth to adulthood, doubling in size during this time (Elston et al., 2009b). Pyramidal cells in the granular prefrontal cortex also continue to grow from birth to adulthood (Elston et al., 2009a; Travis et al., 2005). These data suggest that, while the peak in exuberant connections may

* *Corresponding author.*
E-mail address: guyelston@yahoo.com (G.N. Elston).

0006-8993/$ – see front matter © 2009 Elsevier B.V. All rights reserved.
doi:10.1016/j.brainres.2009.12.056

occur relatively early in postnatal development in the macaque (approximately $3^1/_2$ months (Rakic and Kornack, 2001)), neurons continue to refine their connections over an extended period of time. The magnitude of this refinement in connectivity and the period over which it occurs vary considerably in different parts of the cerebral cortex.

However, pyramidal cell development has only been quantified systematically in a handful of cortical areas, less than one tenth of the total number of areas reported in the cortical mantle (see (Felleman and Van Essen, 1991; Kaas, 2005; Northcutt, 2002) for reviews of cortical organization). Here we focus our attention on the primary auditory cortex (A1). A1, like V1, is a primary sensory area; however, unlike V1, A1 receives sensory inputs *in utero*, which have been demonstrated to be essential for the normal development of auditory processing (Mody, 2003; Vouloumanous and Werker, 2007). Thus, it might be reasonable to assume that cortical circuits mature more rapidly in A1 as compared with V1. However, surgical implantation of prosthetic cochlea has been remarkably successful in young children up to ages of 3–4 (Sharma and Dorman, 2006), suggesting that circuit refinement in auditory cortex may occur over an extended period. The present investigation was designed to probe these opposing possibilities.

2. Results

One hundred and seven pyramidal cells injected in layer III of A1 were included for analyses as they had an unambiguous apical dendrite, had their complete basal dendritic trees contained within the section, and were well filled (Table 1). These data are presented and compared with those obtained from one hundred and twenty-five cells from V1 in the right hemisphere of the same animals (Elston et al., 2009a,b) to allow comparisons of the developmental profiles of cells in these two primary sensory areas. Over 14,000 individual dendritic spines in A1 were drawn and tallied.

2.1. *Dendritic tree size*

The basal dendritic trees of pyramidal cells in A1 at 2 days of age ($59.38\times10^3\pm9.47\times10^3$ μm^2, mean±standard deviation) were smaller than those observed at $3^1/_2$ months of age ($69.16\times10^3\pm11.04\times10^3$ μm^2), which were, in turn, smaller than those observed at 7 months of age ($84.91\times10^3\pm13.20\times10^3$ μm^2) (Fig. 1A). Those in the adult ($4^1/_2$ years old) were the smallest of all ($50.55\times10^3\pm7.98\times10^3$ μm^2). The dendritic trees of cells in the adult were less than 60% the size of those observed at

Table 1 – Vital statistics of the animals used in the present study and number of layer III pyramidal cells sampled from the primary auditory (A1) and primary visual (V1) areas that were included for analyses.

Age	Animal	Gender	Body weight (kg)	Number of cells	
				A1	V1 [a]
2D	CI9	male	0.35	21	25
3.5M	CI10	male	0.56	26	29
7M	CI8	male	0.70	27	34
4.5Y	CI12	male	2.74	33	37
Total				107	125

[a] Data sampled from references 14 and 15.

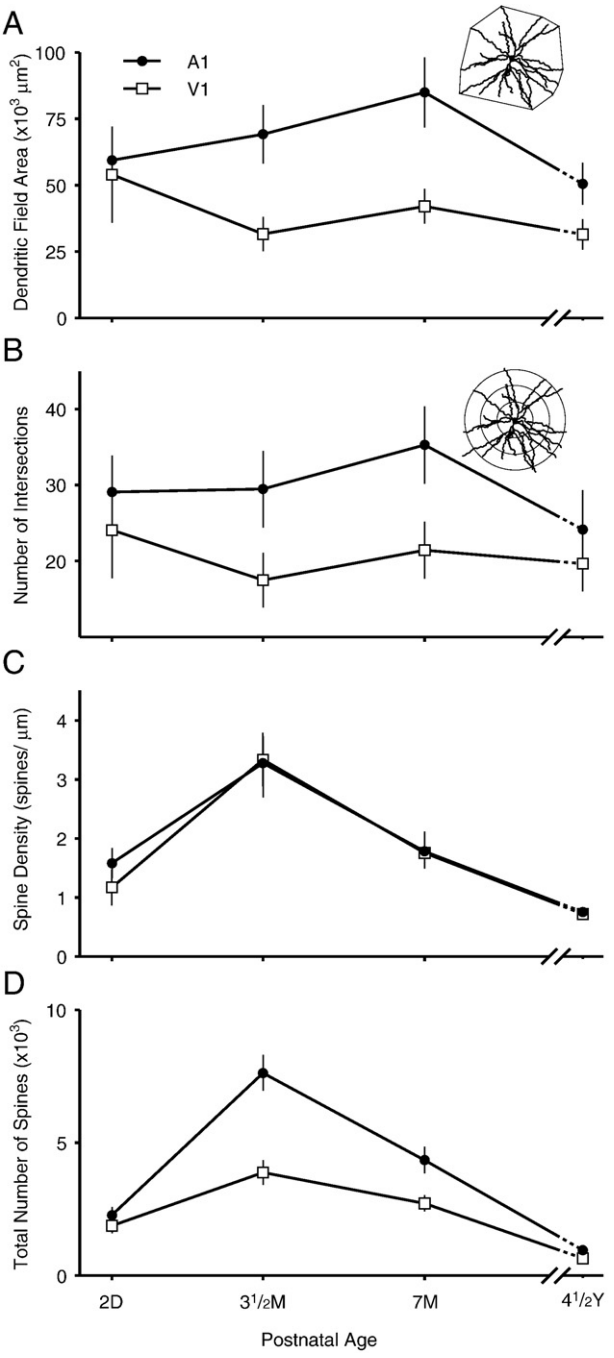

Fig. 1 – Plots of the (A) size of, (B) number of branch points in, (C) the peak spine density along and (D) total number of spines in the basal dendritic trees of layer III pyramidal neurons in the primary auditory cortex (A1) and primary visual cortex (V1). Data were sampled from animals 2 days old (2D), $3^1/_2$ months old ($3^1/_2$M), 7 months old (7M), and $4^1/_2$ years old ($4^1/_2$Y). Error bars = standard deviation.

7 months of age. This profile differed from that observed in V1, where the largest cells were observed at 2 days and they became progressively smaller through infancy into adulthood. Statistical analysis (one-way ANOVAs) revealed that the size of the basal dendritic trees of pyramidal cells in A1 were significantly different ($p<0.05$) across the age groups ($F_{(3)}=56.23$). In addition, the size of the basal dendritic trees was significantly different between A1 and V1 for each different age group (2 days, $p<0.05$; $3^1/_2$ months, $p<0.01$; 7 months, $p<0.01$; $4^1/_2$ years, $p<0.01$; Mann–Whitney *U*-tests). Notably, the dendritic trees of cells in A1 were twice as big as those observed in V1 at $3^1/_2$ months of age.

2.2. *Branching patterns*

Sholl analyses revealed differences in the branching complexity of the dendritic trees of neurons in A1 with aging (Fig. 1B). The peak branching complexity of cells (defined as the maximum number of intersections observed on concentric circles of increasing radii, steps of 25 μm, centred on the cell body) in newborn and $3^1/_2$-month-old animals was less than that in 7-month-old animals (29.10±4.79; 29.54+5.05; 35.33+5.12, respectively). The peak branching complexity of cells in adults (24.15±5.20) was less than that observed in all other animals. Statistical analysis (one-way ANOVAs) revealed significant differences ($p<0.05$) in the branching structure of the basal dendritic trees of pyramidal cells, as revealed by Sholl analyses, across the age groups ($F_{(3)}=14.37$). Cells in A1 had notably more branches than did cells in V1 at corresponding ages (2 days, $p<0.05$; $3^1/_2$ months, $p<0.01$; 7 months, $p<0.01$; $4^1/_2$ years, $p<0.01$; Mann–Whitney *U*-tests).

2.3. *Density and number of spines of the basal dendrites*

The peak spine density at 2 days of age (1.58±0.41 spines/μm) was less than that at $3^1/_2$ months (3.28±0.59 spines/μm) (Fig. 1C). The peak spine density then became progressively lower through 7 months of age (1.78+0.40 spines/μm) to the adult (0.74±0.24 spines/μm) (see Fig. 4 for microphotograph). A repeated measures ANOVA revealed these differences in spine density to be significant ($p<0.05$) across ages ($F_{(3)}=338.46$). This trend was similar to that observed in V1, where the peak spine densities at 2 days, $3^1/_2$ months, 7 months, and $4^1/_2$ years were 1.17±0.33, 3.35±0.50, 1.76±0.28, 0.69±0.19 spines/μm, respectively.

We calculated an estimate for the total number of spines in the basal dendritic tree of the "average" pyramidal neuron in A1 for the different age groups by summing the product of the number of dendritic branches and spine density along the entire extent of the dendritic tree (see (Elston, 2001)). These calculations revealed a considerable increase in the number of spines in the basal dendritic trees of cells in A1 from 2 days (2,280) to $3^1/_2$ months of age (7,630) (Fig. 1D). At 7 months of age, cells in A1 had 4,344 spines in the basal dendritic trees, more than observed in the adult (943). This trend was similar to that observed in V1; however, cells in A1 acquired approximately 5,300 spines from 2 days to 3-$^1/_2$ months of age, whereas cells in V1 acquired approximately 2,000 spines over this same period. Thus, cells in A1 grew at least $2^1/_2$ fold more spines in their basal dendritic trees than did those in V1.

3. Discussion

Here we investigated the morphology of layer III pyramidal cells of the primary auditory area (A1) in monkeys aged 2 days to $4^1/_2$ years old. We found that, while peak spinogenesis was observed at $3^1/_2$ months of age (see also (Bourgeois and Goldman-Rakic, 1993; Bourgeois et al., 1994; Lidow et al., 1991; Zecevic et al., 1989; Zecevic and Rakic, 1991)), the basal dendritic trees of pyramidal cells in A1 continued to grow beyond this peak until at least 7 months of age. Likewise, the dendritic trees continued to form more branches up to at least 7 months of age. Comparison of these data with those sampled from the primary visual area (V1) of the same animals (Elston et al., 2009a,b) reveals that cells in these two different primary sensory areas have different growth profiles. Whereas the basal dendritic trees of cells in A1 continued to grow for at least 7 months after birth, those in V1 decreased in size after birth. Cells in A1 continued to grow new branches until at least 7 months of age, the same does not hold for cells in V1. At their peak ($3^1/_2$ months of age), cells in A1 had twice the number of spines in their dendritic trees as did those in V1 (7,630 and 3,883, respectively).

The present data suggest that pyramidal cells in A1 are not characterised by precocial development, as may reasonably have been assumed by virtue of their prenatal sensory experience (Mody, 2003) and early myelination (Flechsig, 1920). On the contrary, the present data suggest that pyramidal cells in A1 undergo a protracted period of circuit refinement through dendritic growth and the formation of new branches as compared with V1. Clearly, new spines grow on these new dendritic processes at a time when there was a net reduction in the number of spines/synapses in cortex (i.e., the new branches are studded in spines, most of which have been demonstrated to have at least one excitatory synapse in mature cortex (Arellano et al., 2007)). In some respects, the present data for A1 pyramidal cell development more closely approximates that reported in high-level sensory association cortex than V1. For example, pyramidal cells in A1, like those in inferotemporal cortex, which are involved in processing global aspects of the visual scene (Fujita, 2002; Tanaka, 1996), continue to grow in size and increase in branching complexity from 2 days old throughout infancy to 7 months of age, consistent with the increased metabolic rate observed in the developing monkey cerebral cortex during this time (Jacobs et al., 1995). Similar findings have been reported in the human cerebral cortex (Conel, 1941, 1947, 1955, 1959, 1963, 1967; Shadé and van Groenigen, 1961). Cells in V1 of the macaque, on the other hand, decrease in size over this same period (Fig. 2). It is also worth noting that cells in A1 in the adult macaque brain are larger, more branched and more spinous than those in V1.

As reviewed in detail elsewhere (Elston, 2007; Häusser et al., 2000; Jacobs and Scheibel, 2002; Koch, 1999; Spruston, 2008), differences in the morphology of pyramidal cell's dendritic trees may influence various aspects of cortical function. In particular, Poirazi and Mel (2001) proposed that

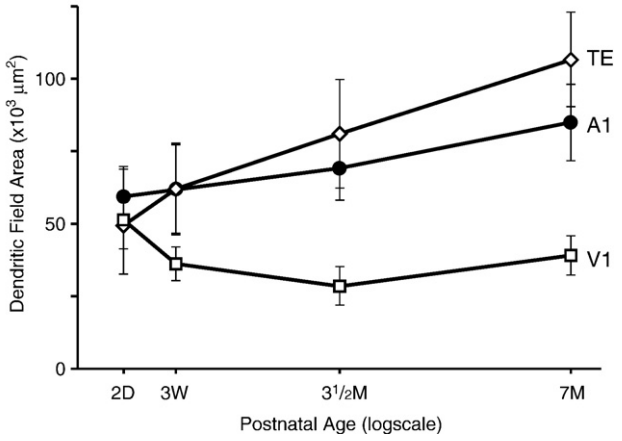

Fig. 2 – Graph illustrating the size of the basal dendritic trees of layer III pyramidal cell in the primary auditory area (A1), the primary visual area (V1), and visual association area TE from animals 2 days old (2D), $3^1/_2$ months old ($3^1/_2$M), and 7 months old (7M). Note that the dendritic trees of cells in A1 and TE continue to grow in size from 2 days to 7 months of age while those in V1 become smaller during this same period. Error bars = standard deviation.

the number and spatial distribution of inputs within the dendritic tree influence the functional capacity of individual pyramidal cells. Likewise, differences in the number of spines contained within the dendritic trees, and their branching pattern, reportedly influence the potential for plasticity (see (Chklovskii et al., 2004) for a review). Thus, by virtue of their more branched, more spiny dendritic trees, pyramidal cells in A1 may have a greater functional capacity and greater potential for plasticity during development than do cells in V1. In addition, because the dendritic trees of cells in A1 continue to grow more branches after birth, and grow many more spines than do those in V1, cells in A1 may be characterised by a greater potential for plastic change over a protracted period of time compared with V1.

The present data on the developmental profiles of pyramidal cells in auditory cortex, and the abovementioned theoretical predictions relating neuron structure to function, are consistent with clinical outcomes in hearing impaired children. Remarkable success has been achieved in improving speech perception and language skills in hearing-impaired babies by surgical implantation of cochlear implants (Clark, 2008; Clark et al., 1977). The best results are achieved by intervention up to 3–4 years of age (Fryauf-Bertschy et al., 1997; Kirk et al., 2002; Manrique et al., 2004; Sharma et al., 2002a,b, 2004; Waltzman and Cohen, 1998), when synapse density in A1 is at a peak (Huttenlocher and Dabholkar, 1997). Beyond this age there is a decline in synapse density and auditory cortex appears to be less adept to rewire following implantation (Sharma et al., 2002a,b, 2004, 2005). It remains to be determined how neurotrophic delivery devices (e.g., (Richardson et al., 2009)) or stem cell therapy (e.g., (Nakagawa et al., 2008; Nishimura et al., 2009; Okita et al., 2007)) may expand the temporal window for successful therapeutic treatment of deafness by influencing neurite growth and circuit formation in the adult auditory cortex.

4. Conclusions

The present findings suggest that pyramidal cells in the primary auditory area are characterised by different growth profiles as compared with those in the primary visual area. The dendritic trees of pyramidal cells in A1 continue to grow for at least 7 months after birth, whereas cells in V1 become progressively smaller during this time. Pyramidal cells in A1 attain almost double the number of spines in their dendritic trees than do those in the primary visual area. In some respects, the developmental growth profiles of pyramidal cells in A1 of the macaque monkey more closely reflected those in high order association cortex, regions associated with protracted development and high levels of plasticity. In future studies it will be worthwhile to include a larger number of animals for study, neurones from other cortical layers and animals of different ages to better comprehend the heterogeneity of developmental profiles in the cerebral cortex.

5. Experimental procedures

Four male macaque monkeys (*Macaca fascicularis*) were used in the present study (Table 1). Animals ranged in age from 2 days old to $4^1/_2$ years old. Three of these animals (CI8, CI9, CI10) are the same as those from which data were sampled in our previous studies in visual and granular prefrontal cortex (Elston et al., 2009a,b), thus allowing direct comparisons among data. We selected these age groups for study specifically because 3 weeks of age correlates with the window of the critical period of ocular dominance shift in the primary visual area (Horton and Hocking, 1997), $3^1/_2$ months of age corresponds to the peak spinogenesis (Bourgeois and Goldman-Rakic, 1993; Bourgeois et al., 1994; Lidow et al., 1991; Zecevic et al., 1989; Zecevic and Rakic, 1991) and the end of the critical period (Horton and Hocking, 1997), 7 months of age corresponds approximately with the period of increased metabolic activity in the cerebral cortex (Jacobs et al., 1995) and four and a half years corresponds to young adulthood. Two days of age was the youngest animal we were able to obtain. The cell injection methodology and immunohistochemical processing employed in the present study has been outlined in detail in previous studies (Buhl and Schlote, 1987; Elston, 2001; Elston and Rosa, 1997). The animals were deeply anaesthetised with sodium pentobarbital (Nembutal, >75 mg/kg i.v. or i.p., Dainippon Sumitomo Pharma, Osaka, Japan) in accordance with protocols approved by Osaka University and regulations for the care and use of animals set out by the NIH (publication No. 86-23, revised 1996), perfused intracardially and the brain removed.

Tissue including A1 was excised from the inferior bank of the lateral sulcus of the left hemisphere. The white matter was trimmed and the remaining grey matter was "flat-mounted" and postfixed overnight between glass slides in a solution of 4% paraformaldehyde in 0.1 M phosphate buffer (PB). Serial thick sections (250 µm) were cut tangential to the cortical surface with the aid of a vibratome. Individual sections were

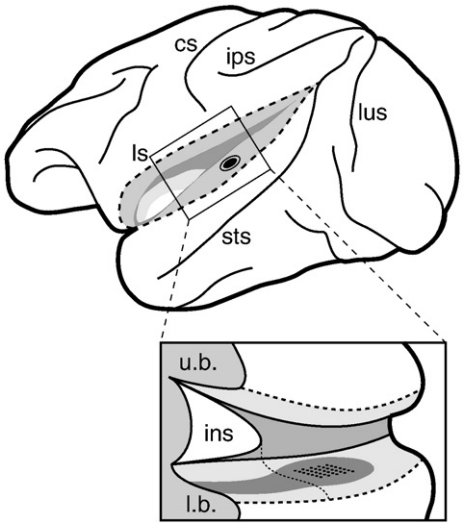

Fig. 3 – Schematic illustrating the gross location of the primary auditory cortical areas in the lateral sulcus and (inset) the region within the lateral sulcus in which neurons were injected. Dots illustrate the region of cortex in which we injected neurons. cs, central sulcus; ips, intraparietal sulcus; ins, insula; ls, lateral sulcus; lus, lunate sulcus; sts, superior temporal sulcus; l.b. and u.b., lower and upperbanks of sts.

incubated in a solution containing 10^{-5} mol/L of the fluorescent dye 4,6 diamidino-2-phenylindole (DAPI; Sigma D9542, St Louis, MO) in PB at room temperature for approximately 10 min and mounted between Millipore filters (AABG02500, Billerica, MA). The slice preparation was then mounted in a perspex dish on a fixed stage microscope (Eclipse FN1, Nikon, Tokyo, Japan) and the preparation visualised with UV excitation (380–420 nm).

Because the number, location and nomenclature of auditory areas in the macaque monkey vary according to different reports (see reference (Hackett et al., 1998) for a review), we deliberately selected a particular region within the lateral sulcus identified as A1 across studies (Burton and Jones, 1976; Galaburda and Pandya, 1983; Hackett et al., 1998; Jones et al., 1995; Merzenich and Brugge, 1973; Morel et al., 1993; Pandya and Sanides, 1973). Specifically, we selected for intracellular injection that part of the inferior bank of the lateral sulcus located posteriorly towards the apex of the superior temporal sulcus at which the cortex is often raised into a "bump" (Fig. 3). In all cases, we sampled cells half way between the exposed portion of the gyrus and the insula at the level of this "bump" in a bid to maximize the possibility that we injected neurones in similar regions of the tonotopic representation in the different cases (e.g., (Kosaki et al., 1997; Merzenich and Brugge, 1973; Morel et al., 1993; Rauschecker et al., 1995) (Fig. 3 inset). By employing standard immunohistochemical techniques to reveal parvalbumin in the neuropil (e.g., (DeFelipe et al., 1999)) we were able to confirm that injected cells included for analyses here were located in A1 (see (Kosaki et al., 1997; Morino-Wannier et al., 1992)).

DAPI-labelled neurons were injected under visual guidance with continuous negative current (up to 100 nA). We injected cells with cell bodies located at the base of layer III, immediately above the granular layer IV (Hassler, 1966) so as to be able to make direct comparisons with our other data also

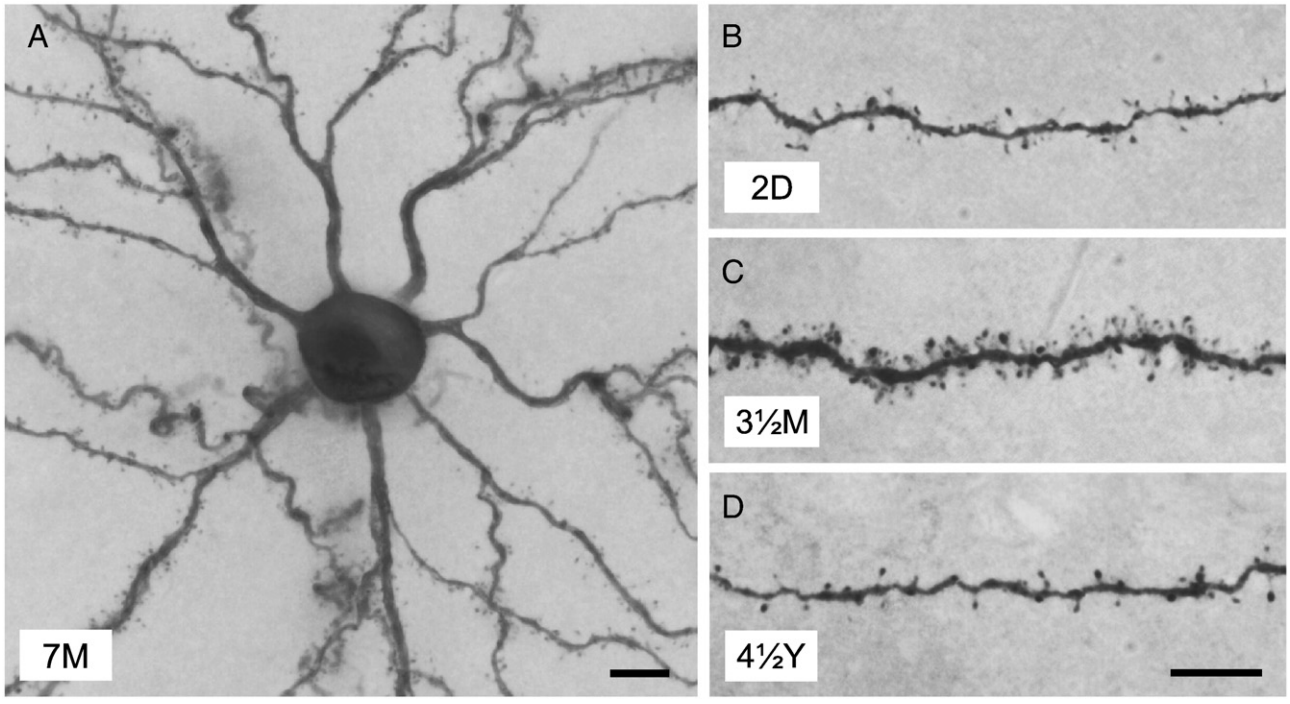

Fig. 4 – (A) Low-power photomicrograph of a layer III pyramidal cell sampled from the primary auditory area that was injected with Lucifer Yellow and processed with a diamino-benzidine reaction product. (B–D) Higher power photos of the basal dendrites of layer III pyramidal cells, revealing their dendritic spines. Note the difference in spine density observed at the different ages. Scale bar = 10 μm.

sampled from layer III (Elston, 2000, 2001; Elston et al., 2005, 2009a, Elston and Rockland, 2002; Elston and Rosa, 1997, 1998; Elston et al., 1999). The border between layers III and IV can be distinguished easily in tangential DAPI-labelled sections by detecting differences in neuronal density and cell body size while focussing through the depth of tissue (e.g., see Fig. 3 of Elston and Rosa (Elston and Rosa, 1997)). Once a suitable number of neurons had been injected, the slice was processed for a light-stable reaction product (Elston and Rosa, 1997). The sections were processed in a solution containing 0.6 μg/ml biotinylated anti-Lucifer Yellow (A-5751, Invitrogen, Carlsbad, CA) in stock solution [2% bovine serum albumin (A3425, Sigma, St. Louis, MO), 1% Triton X-100 (X100, Sigma-Aldrich, St. Louis, MO), 0.1% sodium azide, and 5% sucrose in PB] for 4 to 11 days at room temperature, washed 3 times for 10 min each in PB, incubated in streptavidin-biotinylated horseradish peroxidase complex (1:100; RPN1051, GE Healthcare, Uppsala, Sweden) for 2 h, washed 3 times for 10 min each in PB, then incubated in 0.5% 3,3'-diaminobenzidine tetrahydrochloride (DAB, D5637, Sigma; 1:200 in PB) for 10 min at room temperature before being reacted in a solution containing 1% hydrogen peroxide and 0.5% DAB in PB. This method yields a light-stable robust reaction product (Fig. 4).

The dendritic trees and cell bodies of neurons were reconstructed with the aid of a microscope (Eclipse 80i, Nikon, Tokyo, Japan) equipped with a motorized stage (Ludl Electronic Products, Harthorne, NY) and CCD camera (CX9000, MBF Biosciences, Williston, VT). The size and branching structure of the dendritic trees was determined with the aid of Neurolucida software (MBF Bioscience, Williston, VT). The size of the dendritic trees was determined in the tangential plane as the area contained within a convex hull joining the outermost distal tips of the basal dendrites (Fig. 1A inset; see also Fig. 3 of reference (Elston et al., 2009b)). The branching structure was determined by Sholl analyses (Sholl, 1953). Consistent with our previous publications of neocortical pyramidal cells, all statistical comparisons of dendritic branching structure were made by comparing the number of intersections with corresponding Sholl annuli across groups. All dendritic trees were reconstructed by the same individual (TO).

Spine densities were calculated from high-power (Nikon ×100 oil immersion objective N.A. 1.40) reconstructions of individual dendrites drawn with the aid of a camera lucida, consistent with all previous publications by GNE. Specifically, we drew twenty horizontally-projecting dendrites, in their entirety, selected from randomly selected cells in each animal. The number of spines was then tallied per successive 10 μm segment of dendrite from the cell body to the distal tip to determine spine density as a function of distance along the dendrite (Eayrs and Goodhead, 1959; Valverde, 1967). Horizontally-projecting dendrites were selected to avoid trigonometric error. Consistent with our previous publications of neocortical pyramidal cells, all statistical comparisons of spine density were made by comparing spine density as a function of distance from the soma to the distal tips of the dendrites. All spines were drawn and no distinction was made between different spine types (e.g., (Jones and Powell, 1969)). All spines were drawn by the same individual (GNE).

Acknowledgments

Supported by grants from the Japan Science and Technology Agency (Core Research for Evolutional Science and Technology), Osaka University, the Ministry of Education, Culture, Sports, Science, and Technology (17022025), and I Hear Innovation, Hear and Say (Australia). Address correspondence and reprint requests to Guy Elston at Centre for Cognitive Neuroscience, 60 Duke Rd, Doonan, Qld 4562, Australia.

REFERENCES

Arellano, J.I., Espinosa, A., Fairen, A., Yuste, R., DeFelipe, J., 2007. Non-synaptic dendritic spines in neocortex. Neuroscience 145, 464–469.

Bourgeois, J.-P., Goldman-Rakic, P.S., 1993. Changes of synaptic density in the primary visual cortex of the macaque monkey from fetal to adult stage. J. Neurosci. 13, 2801–2820.

Bourgeois, J.-P., Goldman-Rakic, P.S., Rakic, P., 1994. Synaptogenesis in the prefrontal cortex of rhesus monkeys. Cereb. Cortex 4, 78–96.

Buhl, E.H., Schlote, W., 1987. Intracellular Lucifer yellow staining and electronmicroscopy of neurones in slices of fixed epitumourous human cortical tissue. Acta Neuropathol. 75, 140–146.

Burton, H., Jones, E.G., 1976. The posterior thalamic region and its cortical projection in New World and Old World monkeys. J. Comp. Neurol. 168, 249–302.

Chklovskii, D.B., Mel, B.W., Svoboda, K., 2004. Cortical rewiring and information storage. Nature 431, 782–788.

Clark, G.M., 2008. Personal reflections on the multichannel cochlear implant and a view of the future. J. Rehabil. Res. Dev. 45, 651–693.

Clark, G.M., O'Laughlin, B.J., Rickards, F.W., Tong, Y.C., Williams, A.J., 1977. The clinical assessment of cochlear implant patients. J. Laryngol. Otol. 91, 697–708.

Conel, J.L., 1941. The cortex of a one month old infant. The Post Natal Development of the Human Cerebral Cortex, Vol. II. Harvard University Press, Cambridge.

Conel, J.L., 1947. The cortex of a three month old infant. The Post Natal Development of the Human Cerebral Cortex, Vol. III. Harvard University Press, Cambridge.

Conel, J.L., 1955. The cortex of a fifteen month old infant. The Post Natal Development of the Human Cerebral Cortex, Vol. V. Harvard University Press, Cambridge.

Conel, J.L., 1959. The cortex of a twenty-four month old infant. The Post Natal Development of the Human Cerebral Cortex, Vol. VI. Harvard University Press, Cambridge.

Conel, J.L., 1963. The cortex of a four year old child. The Post Natal Development of the Human Cerebral Cortex, Vol. VII. Harvard University Press, Cambridge.

Conel, J.L., 1967. The cortex of a six year old child. The Post Natal Development of the Human Cerebral Cortex, Vol. VIII. Harvard University Press, Cambridge.

DeFelipe, J., Fariñas, I., 1992. The pyramidal neuron of the cerebral cortex: morphological and chemical characteristics of the synaptic inputs. Prog. Neurobiol. 39, 563–607.

DeFelipe, J., González-Albo, M.C., del Río, M.R., Elston, G.N., 1999. Distribution and patterns of connectivity of interneurons containing calbindin, calretinin and parvalbumin in visual areas of the occipital and temporal lobes of the macaque monkey. J. Comp. Neurol. 412, 515–526.

Eayrs, J.T., Goodhead, B., 1959. Postnatal development of the cerebral cortex in the rat. J. Anat. 93, 385–402.

Elston, G.N., 2000. Pyramidal cells of the frontal lobe: all the more spinous to think with. J. Neurosci. 20 RC95(1-4).

Elston, G.N., 2001. Interlaminar differences in the pyramidal cell phenotype in cortical areas 7m and STP (the superior temporal polysensory area) of the macaque monkey. Exp. Brain Res. 138, 141–152.
Elston, G.N., 2007. Specializations in pyramidal cell structure during primate evolution. In: Kaas, J.H., Preuss, T. (Eds.), Evolution of Nervous Systems, Vol. 4. Academic Press, Oxford, pp. 191–242.
Elston, G.N., Rosa, M.G.P., 1997. The occipitoparietal pathway of the macaque monkey: comparison of pyramidal cell morphology in layer III of functionally related cortical visual areas. Cereb. Cortex 7, 432–452.
Elston, G.N., Rosa, M.G.P., 1998. Morphological variation of layer III pyramidal neurones in the occipitotemporal pathway of the macaque monkey visual cortex. Cereb. Cortex 8, 278–294.
Elston, G.N., Rockland, K., 2002. The pyramidal cell of the sensorimotor cortex of the macaque monkey: phenotypic variation. Cereb. Cortex 10, 1071–1078.
Elston, G.N., Tweedale, R., Rosa, M.G.P., 1999. Cortical integration in the visual system of the macaque monkey: large scale morphological differences of pyramidal neurones in the occipital, parietal and temporal lobes. Proc. R. Soc. Lond. Ser. B 266, 1367–1374.
Elston, G.N., Benavides-Piccione, R., DeFelipe, J., 2005. A study of pyramidal cell structure in the cingulate cortex of the macaque monkey with comparative notes on inferotemporal and primary visual cortex. Cereb. Cortex 15, 64–73.
Elston, G.N., Oga, T., Fujita, I., 2009a. Spinogenesis and pruning scales among functional hierarchies. J. Neurosci. 29, 3271–3275.
Elston, G.N., Oga, T., Okamoto, T., Fujita, I., 2009b. Spinogenesis and pruning from early visual onset to adulthood: an intracellular injection study of layer III pyramidal cells in the ventral visual cortical pathway of the macaque monkey. Cereb. Cortex. doi:10.1093/cercor/bhp203.
Felleman, D.J., Van Essen, D.C., 1991. Distributed hierarchical processing in primate cerebral cortex. Cereb. Cortex 1, 1–47.
Flechsig, P., 1920. Anatomie des menschlichen Gehirns und Rückenmarks, auf Myelogenetischer Grundlage. Thieme, Leipzig.
Fryauf-Bertschy, H., Tyler, R.S., Kelsay, D.M.R., Gantz, B.J., Woodworth, G.G., 1997. Cochlear implant use by prelingually deafened children: the influences of age at implant and length of device use. J. Speech Lang. Hear. Res. 40, 183–199.
Fujita, I., 2002. The inferior temporal cortex: architecture, computation and representation. J. Neurocytol. 31, 359–371.
Galaburda, A.M., Pandya, D.N., 1983. The intrinsic, architectonic and connectional organization of the superior temporal region of the rhesus monkey. J. Comp. Neurol. 221, 169–184.
Hackett, T.A., Stepniewska, I., Kaas, J.H., 1998. Subdivisions in auditory cortex and ipsilateral cortical connections of the parabelt auditory cortex in macaque monkeys. J. Comp. Neurol. 394, 475–495.
Hassler, R., 1966. Comparative anatomy of the central visual system in day- and night-active primates. In: Hassler, R., Stephen, H. (Eds.), Evolution of the forebrain. Thieme, Stuttgart, pp. 419–434.
Häusser, M., Spruston, N., Stuart, G.J., 2000. Diversity and dynamics of dendritic signalling. Science 290, 739–744.
Horton, J.C., Hocking, D.R., 1997. Timing of the critical period for plasticity of ocular dominance columns in macaque striate cortex. J. Neurosci. 17, 3684–3709.
Huttenlocher, P.R., Dabholkar, A.S., 1997. Regional differences in synaptogenesis in human cerebral cortex. J. Comp. Neurol. 387, 167–178.
Jacobs, B., Scheibel, A.B., 2002. Regional dendritic variation in primate cortical pyramidal cells. In: Schüz, A., Miller, R. (Eds.), Cortical Areas: Unity And Diversity. Taylor and Francis, London, pp. 111–131.
Jacobs, B., Chugani, H.T., Allada, V., Chen, S., Phelps, M.E., Pollack, D.B., Raleigh, M.J., 1995. Developmental changes in brain metabolism in sedated rhesus macaques and vervet monkeys revealed by positron emission tomography. Cereb. Cortex 5, 222–223.
Jones, E.G., Powell, T.P.S., 1969. Morphological variations in the dendritic spines of the neocortex. J. Cell Sci. 5, 509–529.
Jones, E.G., Dell'Anna, M.E., Molinari, M., Rausell, E., Hashikawa, T., 1995. Subdivisions of macaque monkey auditory cortex revealed by calcium-binding protein immunoreactivity. J. Comp. Neurol. 362, 153–170.
Kaas, J., 2005. From mice to men: the evolution of the large, complex human brain. J. Biosci. 30, 155–165.
Kirk, K.I., Miyamoto, R.T., Lento, C.L., Ying, E., O'Neill, T., Fears, B., 2002. Effects of age at implantation in young children. Annal. Otol. Rhinol. Laryngol. Suppl. 189, 69–73.
Koch, C., 1999. Biophysics of computation. Information Processing in Single Neurons. Oxford University Press, New York, pp. 413–422.
Kosaki, H., Hashikawa, T., He, J., Jones, E.G., 1997. Tonotopic organization of auditory cortical fields delineated by parvalbumin immunoreactivity in macaque monkeys. J. Comp. Neurol. 386, 304–316.
Lidow, M.S., Goldman-Rakic, P.S., Rakic, P., 1991. Synchronized overproduction of neurotransmitter receptors in diverse regions of the primate cerebral cortex. Proc. Natl. Acad. Sci. U.S.A. 88, 10218–10221.
Manrique, M., Cervera-Paz, F.J., Huarte, A., Molina, M., 2004. Advantages of cochlear implantation in prelingual deaf children before 2 years of age when compared with later implantation. Laryngoscope 114, 1462–1469.
Merzenich, M.M., Brugge, J.F., 1973. Representation of the cochlear partition on the superior temporal plane of the macaque monkey. Brain Res. 50, 275–296.
Mody, M., 2003. Phonological basis in reading disability: a review and analysis of the evidence. Reading and Writing 16, 21–39.
Morel, A., Garraghty, P.E., Kaas, J.H., 1993. Tonotopic organization, architectonic fields, and connections of auditory cortex in macaque monkeys. J. Comp. Neurol. 335, 437–459.
Morino-Wannier, P., Fujita, S.C., Jones, E.G., 1992. GABAergic neuronal populations in monkey primary auditory cortex defined by co-localized calcium binding proteins and surface antigens. Exp. Brain Res. 88, 422–432.
Nakagawa, M., Koyanagi, M., Tanabe, K., Takahashi, K., Ichisaka, T., Aoi, T., Okita, K., Mochiduki, Y., Takizawa, N., Yamanaka, S., 2008. Generation of induced pluripotent stem cells without Myc from mouse and human fibroblasts. Nat. Biotechnol. 1, 101–106.
Nishimura, K., Nakagawa, T., Ono, K., Ogita, H., Sakamoto, T., Yamamoto, N., Okita, K., Yamanaka, S., Ito, J., 2009. Transplantation of mouse induced pluripotent stem cells into the cochlea. NeuroReport 20, 1250–1254.
Northcutt, R.G., 2002. Understanding vertebrate brain evolution. Integ. Comp. Biol. 42, 743–756.
Okita, K., Ichisaka, T., Yamanaka, S., 2007. Generation of germline-competent induced pluripotent stem cells. Nature 448, 313–317.
Pandya, D.N., Sanides, F., 1973. Architectonic parcellation of the temporal operculum in rhesus monkey and its projection pattern. Z. Anat. Entwicklungsgesch 139, 127–160.
Poirazi, P., Mel, B.W., 2001. Impact of active dendrites and structural plasticity on the storage capacity of neural tissue. Neuron 29, 779–796.
Rakic, P., Kornack, D.R., 2001. Neocortical expansion and elaboration during primate evolution: a view from neuroembroyology. In: Falk, D., Gibson, K.R. (Eds.), Evolutionary Anatomy of the Primate Cerebral Cortex. Cambridge University Press, Cambridge, UK, pp. 30–56.
Rauschecker, J.P., Tian, B., Hauser, M., 1995. Processing of complex sounds in the macaque nonprimary auditory cortex. Science 268, 111–114.

Richardson, R.T., Wise, A.K., Thompson, B.C., Flynn, B.O., Atkinson, P.J., Fretwell, N.J., Fallon, J.B., Wallace, G.G., Shepherd, R.K., Clark, G.M., O'Leary, S.J., 2009. Polypyrrole-coated electrodes for the delivery of charge and neurotrophins to cochlear neurons. Biomaterials 30, 2614–2624.

Shadé, J.P., van Groenigen, W.B, 1961. Structural organization of the human cerebral cortex. I. maturation of the middle frontal gyrus. Acta Anat. 47, 74–111.

Sharma, A., Dorman, M., Spahr, A.J., 2002a. A sensitive period for the development of the central auditory system in children with cochlear implants: Implications for age of implantation. Ear and Hearing 23, 532–539.

Sharma, A., Dorman, M.F., Spahr, A.J., 2002b. Rapid development of cortical auditory evoked potentials after early cochlear implantation. Neuroreport 13, 1365–1368.

Sharma, A., Tobey, E., Dorman, M., Martin, K., Gilley, P., Kunkel, F., 2004. Central auditory maturation and babbling development in infants with cochlear implants. Arch. Otolaryngol. Head Neck Surg. 130, 511–516.

Sharma, A., Martin, K., Roland, P., Bauer, P., Sweeney, M.H., Gilley, P., Dorman, M., 2005. P1 latency is a bio-marker for central auditory development in children with hearing impairment. J. Amer. Acad. Audiol. 16, 564–573.

Sharma, A., Dorman, M., 2006. Central auditory development in children with cochlear implants: Clinical implications. Recent Adv. Otorhinolaryngol. 64, 66–68.

Sholl, D.A., 1953. Dendritic organization in the neurons of the visual and motor cortices of the cat. J. Anat. 87, 387–406.

Spruston, N., 2008. Pyramidal neurons: dendritic structure and synaptic integration. Nat. Rev. Neurosci. 452, 420–421.

Tanaka, K., 1996. Inferotemporal cortex and object vision. Ann. Rev. Neurosci. 19, 109–139.

Travis, K., Ford, K., Jacobs, B., 2005. Regional dendritic variation in neonatal human cortex: a quantitative Golgi study. Devel. Neurosci. 27, 277–287.

Valverde, F., 1967. Apical dendritic spines of the visual cortex and light deprivation in the mouse. Exp. Brain Res. 3, 337–352.

Vouloumanous, A., Werker, J.F., 2007. Listening to language at birth: evidence for a bias for speech in neonates. Devel. Science 10, 159–164.

Waltzman, S.B., Cohen, N.L., 1998. Cochlear implantation in children younger than 2 years old. Am. J. Otol. 19, 158–162.

Zecevic, N., Bourgeois, J.P., Rakic, P., 1989. Changes in synaptic density in motor cortex of rhesus monkey during fetal and postnatal life. Brain Res. Dev. Brain Res. 50, 11–32.

Zecevic, N., Rakic, P., 1991. Synaptogenesis in monkey somatosensory cortex. Cereb. Cortex 1, 510–523.